Linearisation of electrically stimulated muscles by feedback control of the muscular recruitment measured by evoked EMG

Christian Klauer[1] Jörg Raisch[1,2] Thomas Schauer[1]
[1]Control Systems Group, Technische Universität Berlin, Germany
[2]Systems and Control Theory Group, Max Planck Institute for Dynamics of Complex Technical Systems, Magdeburg, Germany

***Abstract*— A novel feedback control method for neuro-prosthetic systems is presented which linearises the static input nonlinearity of muscles that are artificially activated by Functional Electrical Stimulation (FES). The proposed method controls the activation state (sum of recruited motor units by FES) of the paralysed muscle. This muscle recruitment state is measured by the FES evoked electromyogram (eEMG). Compared to standard control approaches, no cumbersome off-line or online identification of the complete nonlinear muscle dynamics, often described by Hammerstein or Hill models, and no model inversion are required. The developed approach robustly handles uncertainties and time-variances of the highly nonlinear muscular recruitment behaviour. When building motion control systems for neuro-prostheses, the developed feedback controller should be used at an inner loop receiving command signals (desired muscle activation) from a top level joint-angle control loop. The feasibility of the proposed control scheme has been experimentally demonstrated for the control of the elbow-joint angle in healthy subjects.**

I. Introduction

Functional Electrical Stimulation (FES) is a long proven technique for inducing muscular contractions in patients suffering from upper neuron motor lesion and is often used for rehabilitation purposes or in neuro-prosthesis for restoring lost motor functions [9]. Typically stroke patients and people with spinal cord injury can benefit from FES. The electrical pulses might by applied through electrodes attached to the skin or implanted electrodes. The generated force is modulated by the amplitude and/or pulsewidth of the applied stimuli (spatial recruitment) or by the rate of stimuli (temporal recruitment). In spatial recruitment, the delivered charge, i.e. the product of current amplitude and pulsewidth is important.

The outcome (e.g. the resulting movement) of an applied stimulation pattern is often difficult to predict due to muscular fatigue, spinal and central reflexes, an accommodation behaviour of the muscles (dependence on stimulation history) [11] and the changing physical state of the person. Also slight displacements of the skin electrodes can lead to significant differences in stimulation responses.

Commonly model-based feed-forward and feedback control strategies are used in order generate defined motion trajectories (e.g. [12]). Concerning the neuro-musculo-skeletal models used for control design, there is always a trade-off: More complex models commonly enable a higher control performance, but are often difficult to adapt to the individual subject due to a high experimental effort. Since the process is usually highly time variant, models should be still simple enough to allow for online identification during the application of FES.

An important component of muscle modelling and control is the nonlinear, spatial recruitment curve which describes the number of motor units activated by FES. This static function, depending on the stimulation intensity, is usually modelled as saturation function assuming a linear range for control. Present hysteresis effects are typically neglected for the sake of simplicity. Online identification of this curve is still a challenging task when only input-output data in form of stimulation intensity and joint-angle are available and when more than one muscle acts on one joint.

The control and identification problem greatly simplifies if the output of the recruitment curve is available for measurement. This enables the use of feedback to linearise recruitment behaviour. For designing such a controller only a rough estimate of the average slope is required. This information can be easily aquired (even online) from I/O data of a static curve.

A promising way to gain information on the internal activation state of the stimulated muscle is to analyse the FES evoked Electromyogram (eEMG) [6] which is the electrical response of the muscle to an external electrical stimulus, i.e. the sum of action potentials of all activated motor units. This response is the so-called *M-wave*. By digital filtering of the M-wave after every applied stimulus, a number can obtained that reflects the amount of recruited motor units by the preceding stimulation pulse. In the past, analysis of evoked EMG was used to estimate muscular fatigue [7] or to predict muscular torques [1], [14].

In this paper we go further and make use of the evoked EMG to linearise the motor unit recruitment by feedback. The controller adjusts the intensity of FES according to the measured muscle activation state. Hence, the resulting feedback controlled muscular activation can be approximated by a simple LTI system. This simplifies the entire motion control design to a considerable degree. Furthermore, the effort for parameter identification is reduced in comparison to classical approaches.

Section II gives an overview on the proposed control scheme and the used experimental set-up. The assumed model of the neuro-musculo-skeletal system is described in Section III. In

the following Section IV the feedback control of the muscle recruitment state will be introduced. After this, the top level control for the elbow-joint angle will be discussed in Section V. The applied experimental procedure and obtained results are presented in the Sections VI and VII before the final Section VIII which concludes the development.

II. Control scheme, experimental set-up and EMG processing

The developed control system is exemplary applied the human biceps muscle in order to control the elbow-joint angle against gravity. The proposed control scheme and experimental set-up are shown in Fig. 1. The corresponding M-wave to the previous stimulation pulse with a normalised intensity v (between zero and one) is recorded at a sampling rate of 4kHz using the EMG-amplifier PhysioSense [8]. EMG is recorded from a pair of AgCl electrodes (Neuroline 720, 72000-S/25, Ambu A/S, Denmark) which are located between the two hydro-gel stimulation electrodes (RehaTrode, $4 \times 6.4\,\mathrm{cm}$, HASOMED GmbH, Germany). Fig. 2 illustrates the typical form of evoked EMG for the stimulation periods where k is the index of stimulation pulses. Visible are stimulation artefacts caused by the electrical pulses and the corresponding M-waves whose amplitude depends on the stimulation intensity. For every stimulation period, a digital filter detects the position of the stimulation artefact, performs a windowing from 10 to 50 4kHz-samples after the detected artefact impulse and calculates the variance of the M-wave inside the window. The obtained value $\hat{\lambda}$ correlates with the number of motor units that fired due to the latest stimulation impulse. In a next step, a feedback controller uses the stimulation intensity v to track a given reference signal $r_{\hat{\lambda}}$ for the muscle activation. This control system will be called Recruitment Control (RC).

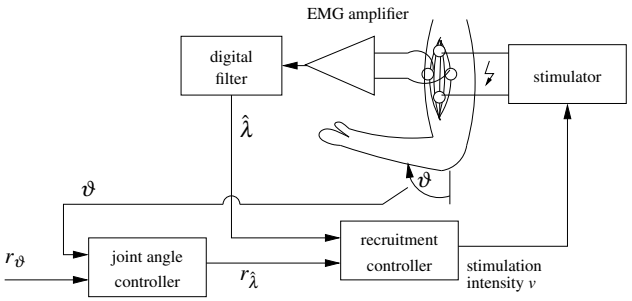

Fig. 1. Experimental set-up and proposed control scheme.

Current amplitude I and pulsewidth pw for the bi-phasic stimulation pulses are obtained from the normalised stimulation intensity v (normalised charge). Current amplitudes in the range of I_{min} =0 mA to I_{max} =90 mA and pulsewidths in the range of $pw_{min} = 0\,\mu$s to $pw_{max} = 500\,\mu$s are possible. Thus a charge $Q = pw \times I$ that ranges from zero to $25\,\mu$C can be realised. This charge is defined for one sub-phase of the bi-phasic pulse. Mapping this charge to the range from zero to one yields the normalised charge $v(k)$ that can be adjusted for each stimulation period k. Current and pulsewidth can also

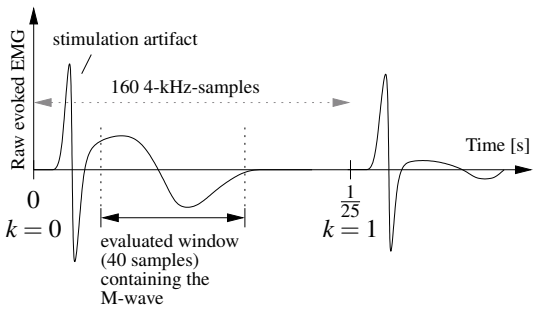

Fig. 2. M-wave occurring after the stimulation pulses.

be normalised between zero and one with respect to their minimal and maximal values. The values of pw and I can be automatically determined from the normalized charge by using a predefined relation between normalised pulsewidth and current amplitude. This approach is called charge control in [13]. One possible realisation is to equally distribute the normalised charge on normalised current amplitude and pulsewidth (linear relation). It should be noted that the resulting functions for the non-normalised current amplitude and pulsewidth are still nonlinear as shown in Fig. 3.

The stimulation pulses are applied to the muscle using the PC-controlled stimulation system RehaStim (HASOMED GmbH, Magdeburg, Germany). A stimulation frequency of 25 Hz is used, i.e. the stimulation period / sampling time for the controller is $T_a = 1/25\,\mathrm{s} = 40\,\mathrm{ms}$.

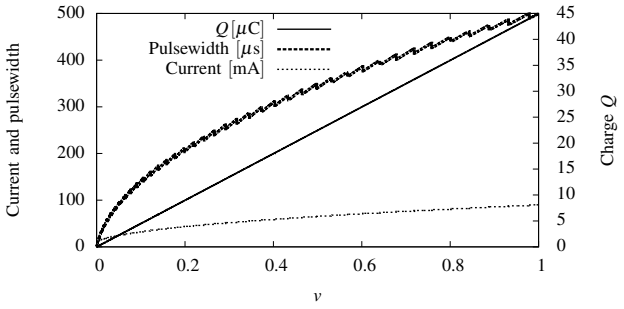

Fig. 3. Current amplitude and pulsewidth of the bi-phasic stimulation pulses as a function of the normalised charge v. Also shown is the charge of one phase of the pulse. The discontinuities in current amplitude and pulsewidth are due to quantisation effects inside the stimulator.

In order to demonstrate the advantage of RC to motion control, an outer cascade position controller is used to generate the reference r_λ for the RC. This top level controller regulates the elbow-joint angle that is measured by an inertial sensor (Sparkfun RazorIMU 9DoF, Sparkfun, United Kingdom) mounted on the lower arm. The sensor/lower arm orientation is obtained by a Direction Cosine Matrix (DCM)-based estimation algorithm [5].

The control system as well as the digital filter are implemented on a PC running Linux with RT-Preemption-Patch. All external devices are connected via USB interfaces. The real-

time dynamic block simulation system OPENRTDYNAMICS[1] is used for implementation of all time critical components and provides a network communication to a QT4-GUI. The design of the control system is carried out with help of the program system SCILAB[2].

III. NEURO-MUSCULO-SKELETAL MODEL

To describe the elbow-joint angle dynamics with FES actuation, a Hill-model [2], succeeded by a second order mechanical system, as shown in Fig. 4 is assumed. The internal muscle recruitment state λ is given by the nonlinear muscular recruitment function $rc(v)$. This function ideally only depends on the stimulation intensity. In reality, there is also a dependence on joint angle and angular velocity as indicated by the dashed line. Also hysteresis effects can be observed. However, for control design this dependence is not considered since it would require an intensive identification effort.

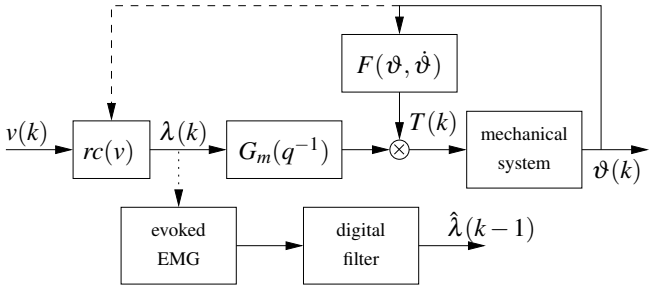

Fig. 4. Assumed neuro-musculo-skeletal system.

An estimate $\hat{\lambda}$ of the internal muscular activation is obtained from the evoked EMG. Since the M-wave occurs after the stimulation pulse, this estimate is only available for usage in the next stimulation period.

In this work, for control design a linear model within an area between a threshold v_{thr} and a maximum tolerable stimulation intensity v_{max} is assumed and estimated by least squares as shown in Fig. 5.

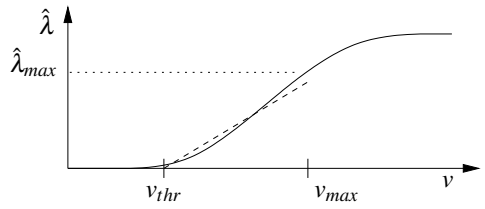

Fig. 5. Sketch of the muscular recruitment curve. The dashed line describes the assumed linear model.

Before controller design, the intensity v_{max} and the corresponding maximal recruitment $\hat{\lambda}_{max}$ are obtained.

Going on in the model description, the activation state is filtered through a 2nd order transfer function G_m that models metabolic processes and typically consists of a time delay of 0.02 s and a low-pass filter with a rise time of 0.04 s [10]. The muscular torque T is then obtained by the product of the transfer function output and the output of a nonlinear function depending on the joint angle ϑ and its derivative. The function F describes the effect of muscle length and contraction velocity on the contractile force of the muscle.

The simplified model describing the relation between the estimated recruitment $\hat{\lambda}$ and the stimulation intensity v for the linear range now consists of linear transfer function model with a time delay of one step:

$$\hat{\lambda}(k) = \Theta_{r,a}\, q^{-1}\, v(k) + \Theta_{r,b} + e(k), \quad v_{thr} \le v(k) \le v_{max} \quad (1)$$

Here, q^{-1} is the backward-shift operator ($v(k)q^{-1} = v(k-1)$) and $e(k)$ is white noise.

IV. RECRUITMENT CONTROL (RC)

The basic idea is to control the recruitment $\hat{\lambda}$ according to the reference $r_{\hat{\lambda}}$. To achieve a good linearisation of the nonlinear recruitment curve and to compensate disturbances the closed-loop bandwidth shall be as large as possible.

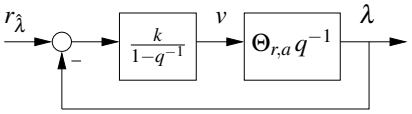

Fig. 6. Recruitment controller applied to the nominal plant.

During control, the offset $\Theta_{r,b}$ of the linear model (1) is treated as a constant disturbance. Therefore, the dynamics from v to $\hat{\lambda}$ can be reduced to a transfer function

$$G(q^{-1}) = \Theta_{r,a}\, q^{-1}.$$

By choosing a discrete-time integrating controller K without time delay,

$$K(q^{-1}) = \frac{k}{1-q^{-1}},$$

the resulting closed-loop behaviour (cf. Fig. 6.) between the reference $r_{\hat{\lambda}}$ and the output $\hat{\lambda}$ is described by

$$T(q^{-1}) = \frac{GK}{1+GK} = \frac{\Theta_{r,a} k\, q^{-1}}{1+(\Theta_{r,a}k-1)\, q^{-1}}.$$

The adjustable closed-loop pole $z_\infty = 1-\Theta_{r,a}k$ (root of closed-loop polynomial $(z+(\Theta_{r,a}k-1))$ in the z-domain describes the closed-loop system performance. The pole location depends on the control gain k. For a desired closed-loop rise time $T_{r,rc}$ and corresponding pole location $z_\infty^{\text{desired}} = e^{-T_a/T_{r,rc}}$ the required gain k can be determined by

$$k = (1-z_\infty^{\text{desired}})/\Theta_{r,a} = (1-e^{-T_a/T_{r,rc}})/\Theta_{r,a}. \quad (2)$$

Here, T_a is the sampling time of the control system. The tuning parameter $T_{r,rc}$ is chosen to maximise the close-loop bandwidth without amplifying system noise.

Since the actuation variable is bounded to the range defined by $v \in [0, v_{max}]$ and because of the integrating controller, an anti-windup strategy as shown in Fig. 7 is used to avoid undesired closed-loop behaviour in case of saturation [3].

[1] http://openrtdynamics.sf.net
[2] http://www.scilab.org

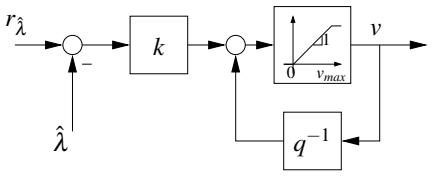

Fig. 7. Recruitment controller with anti-windup strategy.

V. Top level motion control

On top of the RC, the joint-angle feedback controller uses $u_a = r_{\hat{\lambda}}$ as its virtual actuation variable. Since the transfer-function G_m, the nonlinear function F as well as the mechanical model are still undetermined, a LTI system between u_a and the joint angle ϑ is experimentally identified. For excitation, the input signal is changed stepwise. A 2nd order ARX-model [4] without transmission zeros and a time delay of three time steps ($d = 3$) describes the recorded I/O data sufficiently well. Thus the model used for control synthesis is

$$\vartheta(k) = \frac{q^{-d}\mathsf{B}(q^{-1})}{\mathsf{A}(q^{-1})} r_{\hat{\lambda}}(k).$$

with the polynomials A and B defined by

$$\begin{aligned} \mathsf{B}(q^{-1}) &= b_0 \\ \mathsf{A}(q^{-1}) &= 1 + a_1 q^{-1} + a_2 q^{-2}. \end{aligned}$$

Based on this model, a digital polynomial controller is designed using the pole-placement approach [3].

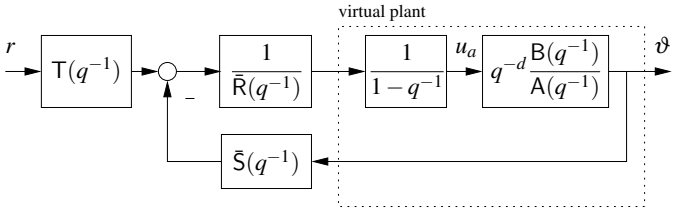

Fig. 8. Digital polynomial controller and virtual plant.

For compensation of stationary control errors, a virtual plant containing the real plant extended by an integrator is used for control design (see Fig. 8). Numerator $\overline{\mathsf{B}}$ and denominator $\overline{\mathsf{A}}$ of the virtual plant are

$$\begin{aligned} \overline{\mathsf{B}}(q^{-1}) &= \mathsf{B}(q^{-1})q^{-d}, \\ \overline{\mathsf{A}}(q^{-1}) &= \mathsf{A}(q^{-1})(1-q^{-1}). \end{aligned}$$

The possible degree of the closed-loop polynomial for a minimal degree controller is determined by the condition

$$\deg(\mathsf{A}_{cl}) \leq \deg(\overline{\mathsf{A}}) + \deg(\overline{\mathsf{B}}) - 1 = 5.$$

The desired closed-loop polynomial for pole-placement is then factorised into two 2nd order polynomials (giving $\deg(\mathsf{A}_{cl}) = 4$):

$$\mathsf{A}_{cl}(q^{-1}) = \mathsf{A}_1(q^{-1}) \cdot \mathsf{A}_2(q^{-1}).$$

Please note, that the closed-loop system will have 5 poles in total in the z-domain. Beside the four poles specified via polynomials $\mathsf{A}_1(q^{-1})$ and $\mathsf{A}_2(q^{-1})$ there will be a fifth pole at the origin. We specify well damped conjugate complex pole pairs for the polynomials $\mathsf{A}_1(q^{-1})$ and $\mathsf{A}_2(q^{-1})$ by the rise times $T_{r,i}, i = 1,2$, and damping values $D_i, i = 1,2$, respectively. The resulting polynomials are given as derived in [3] by

$$\mathsf{A}_i = 1 - 2e^{-D_i\omega_{0,i}T_a}\cos\left(\omega_{0,i}T_a\sqrt{1-D_i^2}\right)q^{-1} + e^{-2D_i\omega_{0,i}T_a}q^{-2},$$

with

$$\omega_{0,i} = \frac{1}{T_{r,i}}\, e^{\frac{D_i}{\sqrt{1-D_i^2}}\cos^{-1}D_i}, i = 1,2.$$

The rise time $T_{r,1}$ is chosen to be smaller than $T_{r,2}$.

For obtaining the controller polynomials $\overline{\mathsf{R}}$ and $\overline{\mathsf{S}}$ (compare Fig. 8) the following Diophantine equation must be solved [3]

$$\overline{\mathsf{A}}(q^{-1})\overline{\mathsf{R}}(q^{-1}) + \overline{\mathsf{B}}(q^{-1})\overline{\mathsf{S}}(q^{-1}) = \mathsf{A}_{cl}(q^{-1}).$$

The pre-filter polynomial T is designed to cancel the factor A_1 of the closed-loop polynomial related to the faster closed-loop dynamics. Additionally, a unity gain of the resulting reference to output behaviour is ensured, yielding

$$\mathsf{T}(q^{-1}) = \frac{\mathsf{A}_1(q^{-1})\mathsf{A}_2(1)}{\mathsf{B}(1)}.$$

A. Sensitivity of the closed-loop

For analysis of the closed-loop behaviour, the sensitivity and the complementary sensitivity function are calculated as

$$\mathcal{S}(q^{-1}) = \frac{\mathsf{R}(q^{-1})\mathsf{A}(q^{-1})}{\mathsf{A}_{cl}(q^{-1})}, \quad \mathcal{T}(q^{-1}) = \frac{\mathsf{B}(q^{-1})\mathsf{S}(q^{-1})}{\mathsf{A}_{cl}(q^{-1})}.$$

with $\mathsf{R} = \overline{\mathsf{R}}(1-q^{-1})$ and $\mathsf{S} = \overline{\mathsf{S}}$.

B. Anti-Windup

For avoiding undesired closed-loop behaviour when the actuation signal saturates, the control structure is modified as proposed in [3] and shown in Fig. 9. If the actuation variable u_a is saturated, a saturation observer prevents integrator windup. The observer polynomial A_{aw} is chosen as

$$\mathsf{A}_{aw}(q^{-1}) = \mathsf{A}_1(q^{-1}).$$

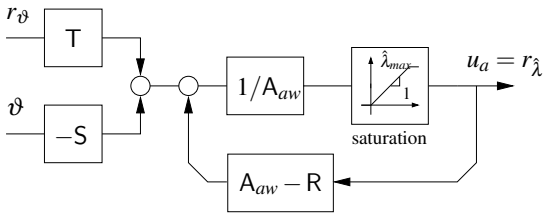

Fig. 9. Implementation of the top level controller to avoid integrator windup.

VI. Experimental Procedure

The following experimental steps are performed:

1) Placement of electrodes and inertial sensor
2) Estimation of v_{max} as well as $\hat{\lambda}_{max}$ according to Sec. III
3) Excitation with $v \in [0, v_{max}]$ while recording $\hat{\lambda}$
4) Least squares estimation of $\Theta_{r,a}$ and $\Theta_{r,b}$ ensuring that $\hat{\lambda} > 0$ for all used I/O data, i.e. $v > v_{thr}$ (cf. Sec. III)
5) Design of the RC (Sec. IV)
6) Excitation of system with RC using a stepwise changing $r_{\hat{\lambda}} \in [0, \hat{\lambda}_{max}]$ while recording ϑ
7) Identification of the ARX model between $r_{\hat{\lambda}}$ and ϑ using the Identification Toolbox for Scilab[3] (Sec. V)
8) Design of the top level angle controller (Sec. V)
9) Verification of the elbow-joint angle controller for a stepwise changing angle reference

VII. Results

The proposed control system was successfully tested on 5 healthy subjects who could not see the reference angle trajectories.

Exemplary data from one subject are presented here. The maximum tolerable stimulation intensity was determined to be $v_{max} = 0.1$ while the maximum of the estimated muscular activation state was $\hat{\lambda}_{max} = 1.6$.

Fig. 10 exemplarily shows ten muscular responses (M-waves) from the open loop experiment performed in Step 3 of the experimental procedure. The stimulation intensity was different for all shown stimulation periods. Data were aligned with respect to the detected stimulation artefacts. Further, stimulation artefacts were blanked between the first and the 10th sample.

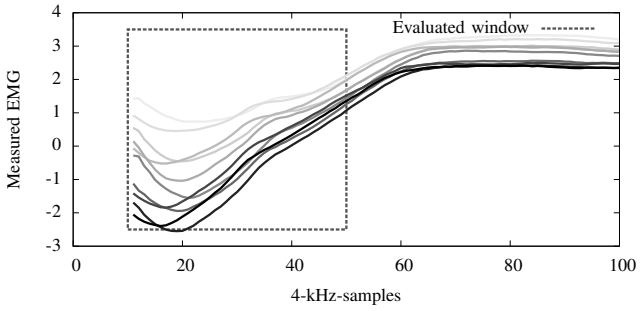

Fig. 10. Set of M-waves from different stimulation periods obtained within an experiment for increasing recruitment. Stimulation artefacts are already cut. The obtained $\hat{\lambda}$ is coded as line colour (brightest line: 0.14, darkest line: 1.55).

Fig. 11 shows the recorded data for identifying the linear relation between the stimulation intensity v and the muscle recruitment $\hat{\lambda}$ as well as the identified linear curve. A large derivation around the fitted curve can be observed. As shown in the lower graph the observed noise level for $\hat{\lambda}$ is less than the derivation from the linear curve observed in the upper plot. This indicates a systematic error. As already outlined in Sec. III this is likely due to a non-modelled dependence on the joint angle and its derivative.

[3] http://atoms.scilab.org/toolboxes/identification/1.1

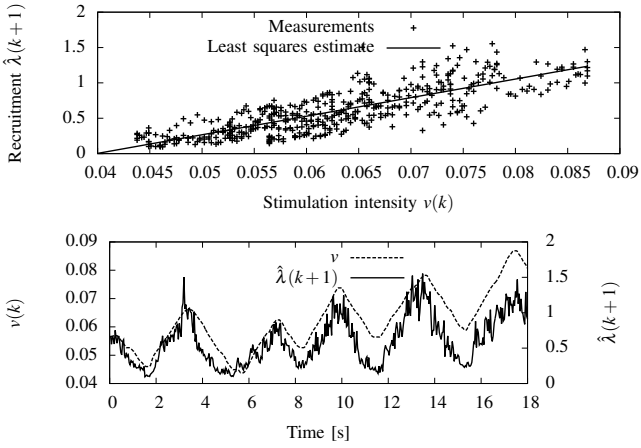

Fig. 11. Identification of the recruitment model (1) using least squares ($\Theta_{r,a} = 26.3$ and $\Theta_{r,b} = -1.04$).

Despite the observed systematic error in the modelling, the feedback control experiment shown in Fig. 12 using the proposed RC shows good tracking results for $\hat{\lambda}$. Hence, the aim of linearising the muscle recruitment by feedback can be achieved with a minimum identification effort. The recruitment controller gain $k = 0.069$ is obtained by means of Eq. (2) for a rise time of $T_{r,rc} = 200\,\text{ms}$.

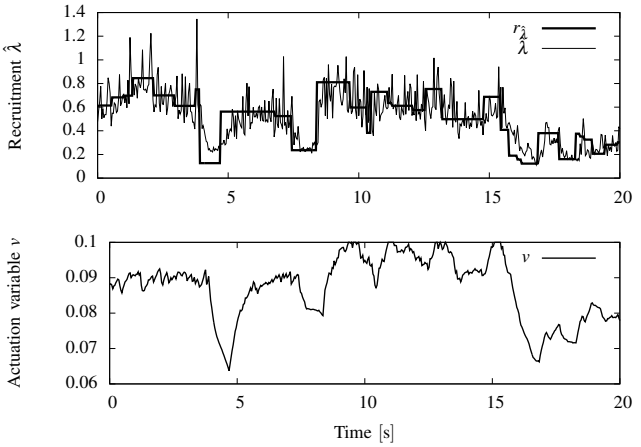

Fig. 12. Evaluation of the recruitment controller (RC).

For design of the top level motion controller the joint-angle dynamics was identified from the data shown in Fig. 13. The measured angle is plotted together with the angle ϑ_{mdl} that is obtained from a simulation using the identified model.

Then, according to Sec. V, the angle controller was parametrised using the rise times $T_{r,1} = 0.6\,\text{s}$, $T_{r,2} = 0.7\,\text{s}$ and dampings $D_1 = D_2 = 0.99$. The amplitudes of the frequency responses for the transfer functions $\mathcal{S}$ and $\mathcal{T}$ are shown in Fig. 14. The small peak of $|\mathcal{S}|$ indicates a robust closed-loop behaviour.

Finally, the elbow-joint angle controller was tested for a stepwise changing angle reference. The result of the test is

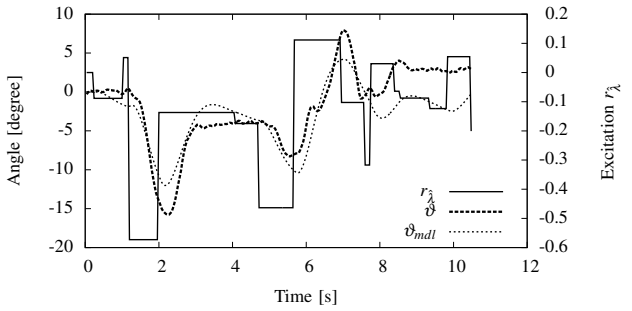

Fig. 13. Identification and validation of the linear model from $r_{\dot{\lambda}}$ to ϑ.

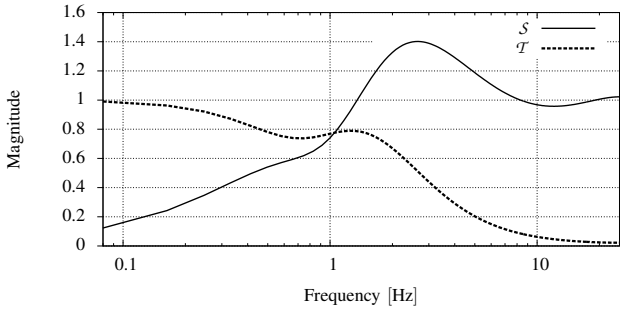

Fig. 14. The frequency responses of the sensitivity $\mathcal{S}$ and the complementary sensitivity $\mathcal{T}$.

shown in Fig. 15 along with the applied stimulation intensity $v(k)$ which is increasing in average over time to compensate muscular fatigue. As observed, the control system enables a good tracking performance with RMS error below 3.37°. The controlled downwards movements show errors caused by voluntary introduced forces due to imperfect relaxation of the healthy subject.

VIII. Conclusions and Outlook

The proposed recruitment controller decreases the effort needed for identification of neuro-musculo-skeletal models when designing controlled neuro-prostheses. The nonlinear static input function (spatial recruitment curve) can be linearised by feedback of the muscle recruitment which is measured by evoked EMG. For the design of the recruitment control system only the slope of the static recruitment curve needs to be identified. This information was obtained in this work by off-line identification. However, the realisation of an on-line identification by recursive least squares should be straightforward. This should enable the implementation of a self-tuning controller.

The obtained angle tracking performance can be furthermore improved by using a nonlinear approach for the top level controller that takes into account the non-linearities inherent to the function F (force-length and force-velocity relation of a muscle) and to the mechanical system.

Future work involves the use of the proposed control strategy for paralysed patients within the European Project MUNDUS to restore arm and hand functions.

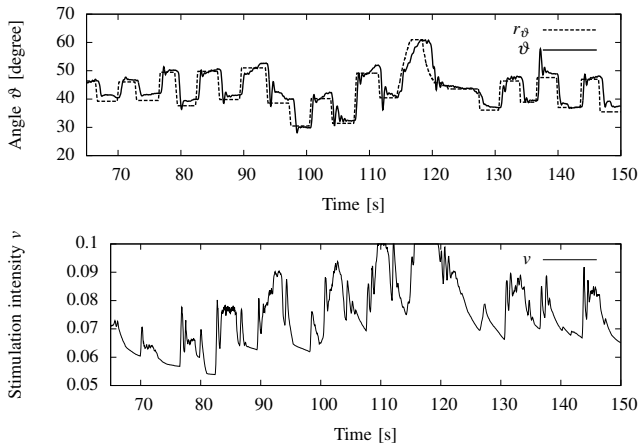

Fig. 15. Results of an joint-angle control experiment for a healthy subject using the underlying recruitment controller.

Acknowledgment

The research leading to these results has received funding from the European Community's Seventh Framework Programme under grant agreement no. 248326 within the project MUNDUS.

References

[1] A. Erfanian, H.J. Chizeck, and R.M. Hashemi. Using evoked EMG as a synthetic force sensor of isometric electrically stimulated muscle. *IEEE Transactions on Biomedical Engineering*, 45(2):188–202, 1998.

[2] A. V Hill. *First and last experiments in muscle mechanics*. Cambridge UP, 1970.

[3] J.A. Karl and B. Wittenmark. *Computer-Controlled Systems: Theory and Design*. Prentice Hall, 1997.

[4] L. Ljung. *System identification*. Prentice Hall, 1999.

[5] R. Mahony, T. Hamel, and J.M. Pflimlin. Nonlinear complementary filters on the special orthogonal group. *IEEE Transactions on Automatic Control*, 53(5):1203–1218, 2008.

[6] R. Merletti and P.A. Parker. *Electromyography: Physiology, engineering, and noninvasive applications*. Wiley-IEEE Press, 2004.

[7] N. Miura, T. Watanabe, and H. Kanai. A Preliminary Study of Muscle Fatigue Evaluation Using M-waves elicted by additional pulses for Rehabilitation with FES. In *Proc. of IFESS 2010*, pages 102–104, 2010.

[8] H. Nahrstaedt, T. Schauer, and R. Seidl. Bioimpedance based measurement system for a controlled swallowing neuro-prosthesis. In *Proc. of IFESS 2010*, pages 49–51, 2010.

[9] P Hunter Peckham and Jayme S Knutson. Functional electrical stimulation for neuromuscular applications. *Annual Review of Biomedical Engineering*, 7:327–360, 2005.

[10] R. Riener and T. Fuhr. Patient-driven control of FES-supported standing up. *IEEE Trans. Rehabil. Eng*, 6(2):113–124, 1998.

[11] D.W. Robbins et al. Postactivation potentiation and its practical applicability: A brief review. *J Strength Cond Res*, 19(2):453–8, 2005.

[12] Riener Robert. Model–based Development of Neuroprostheses for Paraplegic Patients. *Philosophical Transactions of the Royal Society of London. Series B: Biological Sciences*, 354(1385):877–894, May 1999.

[13] R. Shalaby. *Development of an Electromyography Detection System for the Control of Functional Electrical Stimulation in Neurological Rehabilitation*. Doctoral thesis, TU Berlin, 2011.

[14] Q. Zhang, M. Hayashibe, and D. Guiraud. Muscle fatigue tracking based on stimulus evoked EMG and adaptive torque prediction. In *Proc. of IEEE ICRA 2011*, pages 1433–1438. IEEE, 2011.